

# Computational fluid dynamics simulations guided by Fourier velocity encoded MRI

Vinicius Rispoli<sup>1</sup>, Jon-Fredrik Nielsen<sup>2</sup>, Krishna Nayak<sup>3</sup>, and Joao Luiz Carvalho<sup>1</sup>

<sup>1</sup>University of Brasilia, Brasilia, DF, Brazil, <sup>2</sup>University of Michigan, Ann Arbor, MI, United States, <sup>3</sup>University of Southern California, Los Angeles, CA, United States

**Introduction:** Fourier velocity encoding (FVE)<sup>[1]</sup> is a promising MRI method for assessment of cardiovascular blood flow. FVE provides considerably higher signal-to-noise ratio (SNR) than phase contrast (PC) imaging, and is robust to partial-volume effects. On the other hand, FVE does not directly provide velocity maps. These maps are useful for calculating the blood flow through a vessel, or for guiding computational fluid dynamics (CFD) simulations<sup>[2,3]</sup>. PC-driven CFD has been previously demonstrated<sup>[2,3]</sup>, and can be useful for reducing scan time, improving spatial resolution, and/or denoising the MRI data. This work introduces a method for using FVE data (rather than PC data) to guide CFD simulations.

**Methods:** Simulated FVE data was derived from 3DFT FGRE PC data from a pulsatile carotid flow phantom (Phantoms by Design, Inc., Bothell, WA). PC imaging was performed on a 3T GE Discovery MR750 system (50 mT/m, 200 T/m/s), using a 32-channel head coil. Scan parameters: resolution = 0.5×0.5×1.0 mm<sup>3</sup>; FOV = 16×12×7.5 cm<sup>3</sup>; Venc = 50 cm/s; TR = 11.4 ms; flip angle = 8.5°; temporal resolution = 91.2 ms; scan time = 40 minutes; 9 NEX; pulse cycle 60 bpm). The spin-density map (magnitude image),  $m(x,y)$ , and the through-plane velocity map,  $w_{pc}(x,y)$ , corresponding to a temporal frame at mid-systole, were used to simulate a spiral FVE<sup>[4]</sup> spatial-velocity distribution, according to the signal model<sup>[5]</sup>:  $s(x,y,w) = \left[ m(x,y) \cdot \text{sinc} \left( \frac{w-w_{pc}(x,y)}{\delta w} \right) \right] * \text{jinc} \left( \frac{\sqrt{x^2+y^2}}{\delta r} \right)$ , where  $x$  and  $y$

are the in-plane spatial coordinates,  $w$  is the through-plane velocity, and  $\delta r$  and  $\delta w$  are FVE's spatial and velocity resolutions, respectively. The spatial blurring effects of the jinc kernel were reduced using a deconvolution algorithm<sup>[6]</sup> to obtain  $\tilde{s}(x,y,w)$ . Then, an estimate of the true velocity at a given spatial coordinate  $(x_o, y_o)$  was estimated from  $\tilde{s}(x,y,w)$  as<sup>[7]</sup>:  $\hat{w}(x_o, y_o) = \arg \min_{\mu} \left\| \frac{\tilde{s}(x_o, y_o, w)}{m(x_o, y_o)} - \text{sinc} \left( \frac{w-\mu}{\delta w} \right) \right\|_2$ . Finally, CFD calculations were performed using a modified version of the SIMPLER algorithm<sup>[2,3]</sup>, in which  $\hat{w}(x,y)$  was used to constrain the CFD calculation. The phantom's blood-mimicking fluid (viscosity 5 mPa.s, density 1100 kg/m<sup>3</sup>) was assumed to be Newtonian, isothermal, and incompressible. The simulation grid was designed with 0.5×0.5×1.0 mm<sup>3</sup> resolution, and a computational time step  $\delta t = 0.25$  ms was used. Finally, the estimated flow field was compared quantitatively and qualitatively with both a pure CFD solution and the PC-measured flow field. This process was repeated for different values of  $\delta r$  (1 or 2 mm); and for each slice along the  $z$  axis. The velocity resolution,  $\delta w$ , was 10 cm/s.

**Results and Discussion:** The spin-density maps in Fig. 1a illustrate the spatial blurring associated with each value of  $\delta r$ , for a slice perpendicular to the phantom's bifurcation. Fig. 1b presents the FVE-estimated velocity maps,  $\hat{w}$ , for each spatial resolution value, while Fig. 1c shows the associated errors (relative to the PC map,  $w_{pc}$ ). The results show that lower error levels were obtained when FVE data with finer spatial resolution was used. In this slice, the absolute error was greater than 5 cm/s for only 10% of the voxels when  $\delta r = 1$  mm was used; while 31% of the voxels presented error greater than 5 cm/s when  $\delta r = 2$  mm was used. Fig. 2 shows (i) the PC-measured velocity field; and the CFD-simulated velocity fields, obtained using (ii) pure CFD, (iii) FVE-driven CFD ( $\delta r = 1$  mm), and (iv) FVE-driven CFD ( $\delta r = 2$  mm). Considerable qualitative improvement — with respect to agreement with the PC reference — can be appreciated in the FVE-driven results, when compared with the pure CFD result. Table 1 presents the measured signal-to-error ratio (SER) relative to the PC reference, for the CFD results shown in Fig. 2. Both FVE-driven solutions achieved higher SER than the pure CFD approach, when evaluating the three-dimensional velocity vector  $\vec{v} = (u, v, w)$ ; the SER gain (relative to pure CFD) was 1.49 dB when  $\delta r = 1$  mm was used, and 0.80 dB when  $\delta r = 2$  mm was used. When evaluating only the  $y$ -axis velocity component ( $v$ ), there was a 0.11–0.35 dB loss in SER with the proposed method. This may be a positive effect of denoising, since the velocities along that axis are extremely low ( $v_{pc}$ 's total energy is 15.7 dB lower than that of  $w_{pc}$ ). Nevertheless, the SER gains for the  $u$  and  $w$  components more than compensate for this.

**Conclusion:** This work presented a method for using FVE data to guide CFD simulations. We showed that FVE-driven CFD achieves better agreement with a PC-measured velocity map than pure CFD solutions. This is an important result, since a 1-mm resolution spiral FVE dataset could be acquired in the same scan time as 1 NEX of a 0.5-mm resolution PC dataset with the above parameters; however the FVE dataset would have an SNR 23 dB higher than that of PC (for a 2-mm resolution spiral FVE, scan time would be 3 times shorter, and the SNR would still be 8 dB higher than those of PC).

**References:** [1] Moran PR. MRI 1:197. [2] Nielsen JF et al. Proc ISMRM 17:3858, 2009. [3] Rispoli VC et al. Proc ISMRM 22:2490, 2014. [4] Carvalho JLA and Nayak KS. MRM 57:639, 2007. [5] Carvalho JLA, et al. MRM 63:1537, 2010. [6] Krishnan D and Fergus R. Proc 24<sup>th</sup> NIPS, 2009. [7] Rispoli VC and Carvalho JLA. Proc ISMRM 21:68, 2013.

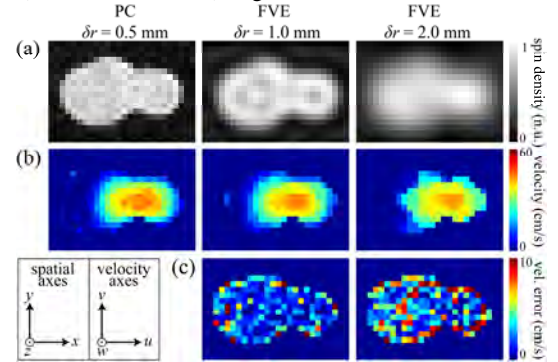


**Figure 1:** (a) Spin-density maps for PC (0.5 mm spatial resolution), FVE with 1 mm spatial resolution, and FVE with 2 mm spatial resolution, for a slice perpendicular to a carotid phantom's bifurcation; (b) corresponding velocity maps; and (c) absolute error for the FVE-estimated velocity maps, relative to the PC reference.

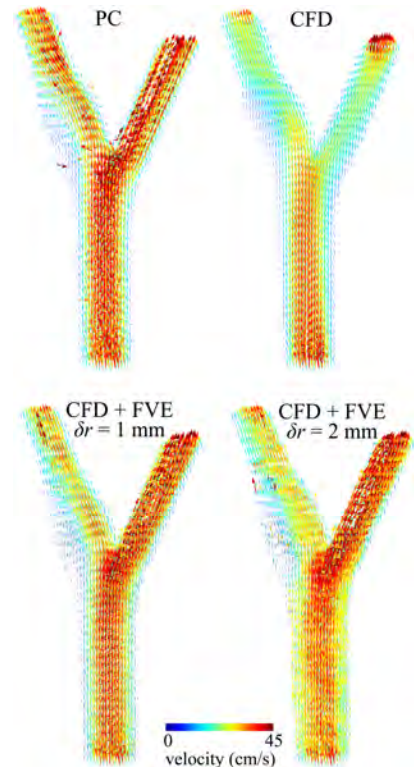


**Figure 2:** 3D visualization of the velocity fields, comparing the PC reference with each CFD approach.

**Table 1:** SER between each of the CFD approaches and the PC reference.

	Pure CFD	CFD + FVE $\delta r = 1$ mm	CFD + FVE $\delta r = 2$ mm
$SER_u$	2.97 dB	3.93 dB (↑)	3.81 dB (↑)
$SER_v$	-0.25 dB	-0.36 dB (↓)	-0.60 dB (↓)
$SER_w$	5.44 dB	10.97 dB (↑)	7.22 dB (↑)
$SER_{\vec{v}}$	6.57 dB	8.06 dB (↑)	7.37 dB (↑)